

Reactions between Molten Iron and Lining Materials

by

E. Kapilashrami, P. Jönsson and S. Seetharaman

Division of Metallurgy, Royal Institute of Technology, Sweden.

ABSTRACT

Erosion of the runners by the flowing molten steel leads not only to increased costs of the refractory lining but also to the contamination of the steel by the products formed. With a view to have an understanding of the mechanism of the chemical corrosion reactions, the present work was initiated. From knowledge of the thermodynamic data available in literature, the stability ranges for various oxide precipitates in the system Fe-O-X where X is Al or Si were mapped. An experimental study of the reaction between molten iron with different oxygen levels and different refractory materials was carried out in which rods of pure, dense Al_2O_3 , SiO_2 and mullite were dipped into molten iron containing different amounts of oxygen contents at 1873°C , over pre-determined time intervals. The rods were then quenched and the cross sections were examined in SEM. Composition profiles were determined by EDS analysis. At the end of each experiment, the oxide content of the molten iron was analysed. From the results, the rate of the reactions was calculated. The mechanism of the reaction is discussed with consideration to refractory lining erosion in the runners.

I. INTRODUCTION

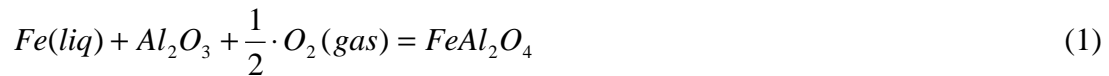
When steel is teemed, the refractory in the runners come under severe attack by the molten steel. This consists of two parts: viz. the chemical corrosion as well as the mechanical erosion wherein the refractory is “peeled” off and the pieces follow the flowing metal. These two phenomena will result in the formation of micro inclusions, macro inclusions and excessive lining wear, leading to the downgrading of the steel quality in terms of steel cleanliness. In order to develop a model that can predict the erosion of the refractory due to chemical reaction, there is a need for understanding nature of these reactions and their mechanisms. Towards this aim, the present work was carried out wherein different refractory materials with well-defined geometry and bulk density were allowed to react with molten iron containing varying amounts of dissolved oxygen under definite time intervals. It was expected that an investigation of the extent of the melt penetration into the refractory and the identification products would throw much light on the reaction mechanisms. To the knowledge of the present authors, very little systematic work has been carried out in this area earlier.

II. THERMODYNAMIC ANALYSIS OF IRON-OXYGEN-REFRACTORY REACTIONS

In order to understand the nature of the erosion reactions, it is imperative to have knowledge of the thermodynamics of the reactions between the refractory materials and oxygen dissolved in liquid iron along with Fe itself. In the present investigations, efforts were focused mainly on two refractory materials, pure alumina and pure silica. It is planned to extend the investigations to mullite and other refractory materials.

II-1. Fe-O-Al system

The phase diagram for the system FeO-Al₂O₃ system is presented in Fig. 1. It is seen that one intermediate compound, viz. FeAl₂O₄. The standard Gibbs energy for the formation of this compound could be obtained from the compilations of Barin.¹



$$\Delta G_1^0 = -327,177 + 81.411 \cdot T \quad kJ \cdot mole^{-1}$$

This was combined with the standard Gibbs energies of solution of oxygen gas (standard state: 1 atm.) taken from literature²

$$\frac{1}{2} O_2(gas, 1atm) = \underline{Q} (1wt\% \text{ solution in Fe}) \quad (2)$$

$$\Delta G_2^0 = -111,070 - 5.87 \cdot T \quad kJ \cdot mole \underline{Q}^{-1}$$

Combining the standard Gibbs energies of reactions (1) and (2), the standard Gibbs energy of formation of $FeAl_2O_4$ due to reaction between liquid Fe, oxygen dissolved in molten iron (1 wt % solution) and pure Al_2O_3 (solid) can be calculated to be



$$\Delta G_3^0 = -216,107 + 87.281 \cdot T \quad kJ \cdot mole^{-1}$$

In a similar way, the standard Gibbs energy of formation of “FeO” (liquid) from molten iron and oxygen saturated iron was taken from literature². From these values, a phase stability diagram was constructed with temperature as a function of wt % oxygen in the system Fe-O-Al. This is presented in Fig. 2. It is clearly seen that at steelmaking temperatures and extremely low oxygen levels in the melt, solid Al_2O_3 is likely to be in equilibrium with liquid iron containing oxygen. At slightly higher oxygen levels, $FeAl_2O_4$ solid would exist up to about 2053 K. This analysis does not consider any eventual solid solution formation between Al_2O_3 and $FeAl_2O_4$. At oxygen saturation levels, liquid “FeO” is likely to be formed along with $FeAl_2O_4$. This would imply that under suitable conditions, there is a likelihood of the formation of $FeAl_2O_4$, probably as an intermediate product during the reaction.

II-2 Fe-O-Si System

The phase diagram for the system FeO-SiO₂ is presented in Fig. 3. The diagram shows that the orthosilicate, Fe_2SiO_4 is formed below 1478 K. The metasilicate, $FeSiO_3$ exists below 1413 K¹. The standard Gibbs energy of formation of these two compounds are taken from Barin’s compilations¹:



$$\Delta G_4^0 = -590,258 + 202.68 \cdot T \quad kJ \cdot mole^{-1} \text{ (T range 1000-1400 K)}$$



$$\Delta G_5^0 = -3,344,480 + 155.82 \cdot T \quad kJ \cdot mole^{-1} \text{ (T range 1000-1400 K)}$$

As both the ortho- as well as the metasilicate are unstable as solids at the steel making temperatures the only solid product that could be formed will be SiO₂. But as the steel cools down, the silicates can be built up at lower temperatures.

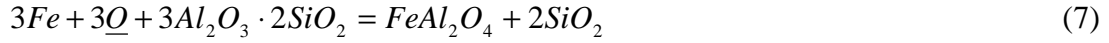
The phase stability diagram for the system Fe-O-Si is presented in Fig. 4.

With regard to mullite, $3Al_2O_3 \cdot 2SiO_2$, the situation is somewhat complicated. This is an extremely stable phase and the standard Gibbs energy of formation of this compound is given by the equation:



$$\Delta G_6^0 = 18,779 - 26.953 \cdot T \quad kJ \cdot mole^{-1}$$

By combining the standard Gibbs energy for reaction (2) with that for reaction (6), the standard Gibbs energy for the reaction between mullite and iron melts containing oxygen was estimated.



$$\Delta G_7^0 = -7,639,430 + 1833.03 \cdot T \quad kJ \cdot mole^{-1}$$

The reactions leading to the formation of $FeSiO_3$ and Fe_2SiO_4 have not been included in the present analysis.

Thus the present thermodynamic analysis indicates that in the case of aluminosilicate refractories, the erosion reactions with aluminosilicate refractories would lead to the precipitation of pure alumina and pure silica particles in the melt. Under higher oxygen levels, the formation of $FeAl_2O_4$ would be favoured.

III. EXPERIMENTAL

III-1. MATERIALS

The carbon-free iron used in the experiments was supplied by ARMCO. This was analysed by X-ray fluorescence analysis and the results³ are presented in Table I. The ARMCO iron was cut into small pieces and heated in hydrogen atmosphere at 973 K for 6 hours in order to remove any surface oxide present before being used in the experiment.

Oxygen was added to the molten iron during the experiments as “FeO”. The wüstite used was synthesised from Fe_2O_3 and iron powder. The Fe_2O_3 of 99.9 % purity, supplied by E. Merck, Darmenstadt, Germany was dried at 383 K for 24 hours. This was then mixed with iron powder, 99.5 % purity also supplied by E. Merck in proper proportions so that the composition of “FeO” produced lies at the Fe/”FeO” phase boundary at 1473 K. The mixing was carried out in an agate ball mill for 1 hour. The powder mixture was then pressed into pellets, placed in an iron crucible with a lid made of iron and was sintered for 24 hours at 1273 K in argon atmosphere. The crucible was then quenched and the “FeO” synthesised were stored in a desiccator. “FeO” thus prepared was subjected to X-ray diffraction analysis (XRD) which showed the absence of metallic iron as well as other oxides of iron. The lattice parameter was evaluated from the XRD analysis was 4.317 Å, which compares well with the value of 4.307 Å given as a reference value in the TADD database.

In the synthesis of “FeO” as well as during the erosion experiments, argon gas was used to protect the system from oxidation. Traces of moisture, CO_2 and oxygen in the commercial Ar gas (supplied by AGA Stockholm. 99.9997 % pure) were removed by letting the gas pass through a gas cleaning system. The moisture in the gas was

removed by passing the gas through columns of silica gel as well as $\text{Mg}(\text{ClO}_4)$. The CO_2 was absorbed by ascarite and the traces of oxygen were removed by passing the gas through copper turnings at 823 K and through magnesium chips at 773 K. It was shown by earlier trials in the present laboratory that the P_{O_2} in the gas thus purified was less than 10^{-18} atm.

Dense rods of Al_2O_3 were supplied by Friatec, Germany. The quartz rods were supplied by Werner Glass, Stockholm. The mullite rods were cut from mullite tubes supplied by Haldenwagner, Germany.

II-2. APPARATUS

The apparatus used for the study of the erosion of refractory materials by molten iron is shown in Fig. 5. An alumina tube was positioned into a vertical tube furnace with Super Kanthal heating elements. The tube was closed with a rubber stopper in the bottom and a water-cooled brass lid, fitted with o-rings to make it gas tight at the top. The rubber stopper at the bottom of the furnace had provision for the inlet of a thermocouple as well as for a gas inlet. Provision was made in the top lid for sampling as well as for the addition of “FeO”, in addition to a gas outlet. Between the lid and the furnace, there was an air lock to prevent air from leaking into the reaction chamber. Purified argon was passed through the furnace. Inside the reaction tube, three radiation shields were placed in the furnace, two in the lower region of the furnace and one in the upper region. Two thermocouples were attached to the furnace; one internal, kept in contact with the bottom of the crucible holding the sample and one external attached to the regulator (Eurotherm) controlling the temperature. The crucible holding the iron sample in the furnace was made out of yttria-stabilised zirconium oxide. The zirconium oxide crucible was placed inside a graphite crucible with molybdenum lining for further protection against any damage due to the cracking of the crucible.

II-3. PROCEDURE

Sufficient quantity of pretreated iron metal (approximately 200 g) was placed in the yttria-stabilised zirconia crucible and the furnace was heated up to 1873 K in argon atmosphere. After ascertaining that all the iron has been molten, wüstite was added into the melt from the top of the furnace to increase the oxygen level in the metal and about 20 minutes were allowed for homogenisation. At this point, a sample of the molten iron was taken out in order to determine the exact amount of dissolved oxygen in the melt. The rods of the different refractory materials were immersed into the melt, through the top of the furnace. The sample holder used is shown in Fig. 6. The rods were allowed to react with the melt for predetermined time intervals after which, they were pulled up to the top of the furnace keeping the argon gas flow high. The rods were then taken out from the furnace and they were subjected to Scanning Electron Microscope Analysis.

III. RESULTS

All the erosion experiments were carried out at 1873 K. The trials with Al_2O_3 rods were run with oxygen levels in molten iron corresponding to 5, 1.91 and 0.2 wt %. At 5 wt % oxygen in iron, the alumina rods were treated for 1, 2 and 5h. When the oxygen content was 1.91 wt %, the treatment times were 1, 2, 10, 24, 36 and 72 h. At the lowest oxygen content in the series, viz. 0.2 wt %, the treatment times were considerably longer, 24, 36 and 72 h.

Only one series of experiments was carried out with quartz rods. The oxygen content in the melt in these experiments was 0.2 wt %. The rods were treated for 24, 36 and 72 h. The experiments with mullite rods are currently being carried out. The results are expected to be ready during the conference.

The result of the SEM analysis of the alumina rods treated in iron melts with 5 wt % oxygen for 2 h is presented in Fig. 7. The dark grey layer is the alumina rod. It is seen that a layer of the reduction product has formed around it. The thickness of the product layer was approximately 80 μm . The reaction appeared to be topochemical. The EDS analysis confirmed that the bulk phase was pure Al_2O_3 . There were a number of bright spots. Compositional analysis of these points showed the presence of iron and oxygen. These islands could be formed due to the penetration of iron containing oxygen through channel defects in the refractory material. The oxygen concentration in these islands seems to be rather high, almost corresponding to stoichiometric FeO considering the analytical uncertainties.

The EDS analysis of the product layer reveals that the product could have an apparent composition 41 at. % Fe, 11 at. % Al and 46 at. % O. Obviously, this corresponds to some sort of a ferroaluminate intermediate product noticed in the counter diffusion of the cations.

Two bright nodular areas are observed clinging to the outer periphery of the product phase. Chemical composition of the drop in the middle of the picture corresponds to nearly 98 % Fe with very little oxygen.

The top bright layer was enlarged and presented in Fig. 8. At point 1, the chemical analysis according to the EDS mapping shows 71 at % Fe, 5 at. % Al and 23 at. % O. The amount of Fe is quite high and the oxygen does not match upto the stoichiometry for FeAl_2O_4 . At the periphery, point 2, there is a further product layer, which is somewhat thin. The chemical composition there corresponds to 27 at % Fe, 16 at. % Al and 55 at. % O. This comes rather close to the FeAl_2O_4 composition.

The EDS analysis of the sample dipped into the iron melt containing 1.91 wt % oxygen for 40 h is shown in Fig. 9. The pattern is somewhat similar to the earlier one. The layer thickness is very little. It is also seen that the layer is chipping off readily during the sample mounting. The chemical composition of the layer was found to be 17 at % Fe, 26 at % Al and 56 at. % oxygen, which would correspond to the phase FeAl_2O_4 .

Fig. 10 shows the SiO_2 reactions with molten iron containing 0.2 % oxygen. The reaction time was 72 h. It was found that the rod was very close to melting and

completely deformed. The EDS analysis in the bulk showed that SiO_2 is likely to be the dominant phase. There were islands due to iron penetration.

IV. DISCUSSION

The iron melt containing 5 wt % oxygen is in the Fe-“FeO” two-phase region. The presence of free “FeO” will accentuate the reaction between the metallic melt and the refractory. The high oxygen levels in the melt would favour the formation of FeAl_2O_4 according to the thermodynamic analysis presented earlier. The ferroaluminate product phase observed in the present experiments is in agreement with this. It is reasonable to surmise the reaction sequence as reaction (3) occurring at the melt-refractory interface. Further penetration of Fe and O should occur through solid state diffusion. The diffusion of the various species through the stoichiometric FeAl_2O_4 phase is expected to be a slow process. The solid state diffusion of MgO and Al_2O_3 through the intermediate spinel phase was investigated by Zhang et al.⁴ The interdiffusion coefficient at 1873 K was reported to be of the order of $4 \cdot 10^{-13} \text{ m}^2/\text{s}$. While the diffusivities in the present case might be higher due to factors like the existence of iron in a higher valency state, the attack could still be considered minimum. Further experiments are currently carried out in order to estimate the diffusivities.

An examination of Fig. 7 reveals that linear cracks are formed in the intermediate layer and they may be likely to propagate with the growth of the layer. If this is the case, there is a likelihood of the product chipping off from the alumina rod and drop into the melt. The melt is expected to contain solid FeAl_2O_4 particles. The metal phase is currently examined for the presence of such particles.

The bright drop of iron sticking to the product layer in Fig. 7 was found to contain very little oxygen. This is quite interesting. Oxygen dissolved in molten iron is surface-active. The interfacial tension between the iron drop and the refractory can be quite low in this case. It is likely that the drop was formed during the quenching of the alumina rod. If the hanging metal drop still reacted with the refractory leading to the formation of ferroaluminate compound, the drop might be depleted in oxygen locally. This would lead to an increase in the contact angle. The bright region above, which contains a higher amount of oxygen, appears to wet the refractory surface well.

Iron melt with 1.9 wt % oxygen would still be in the two-phase region. But the amount of “FeO” present in the melt would be considerably less. This would account for the slow formation of the product layer in contact with Al_2O_3 and its composition being close to stoichiometry. The formation of large grains of this phase and the lesser adhesion to the alumina rod would lead to the inclusion formation in the iron melt.

The reaction between quartz rod and Fe-O melt is very interesting. Fig.10 corresponds to the reaction between SiO_2 and the metallic melt containing 0.2 wt % oxygen. This is very close to the saturation solubility of oxygen in molten iron at the experimental temperature. The sample is close to melting and is well deformed. As the melting point of pure SiO_2 is higher than the experimental temperature, it is difficult to explain the phenomenon unless an intermediate low-melting phase is formed. The Fe-O-Si phase diagram presented in Fig. 3 indicates the existence of the fayalite

($2\text{FeO} \cdot \text{SiO}_2$) phase at lower temperatures. Since this phase decomposes below 1473 K, it is difficult to visualise the formation of fayalite during the reaction. At the present stage, the authors feel that the reaction may proceed by the formation of unstable ternary species, which disintegrate into the metallic melt. This would lead to the formation of silica inclusions in the metal bath.

The reaction between the Fe-O melts and mullite is expected to be a combination of the reactions with quartz as well as alumina. The reaction could be made difficult by the low standard Gibbs energy of formation of mullite. On the other hand, the reaction between SiO_2 and the iron melt containing oxygen indicates that the interaction with mullite is likely to lead to the formation of both Al_2O_3 as well as SiO_2 inclusions in the melt. Further work is being carried out currently to get a deeper insight into these reactions.

The reactions between the runner refractories and iron melts are more complicated. The present work throws some light on the chemical reactions that occur. The commercial ceramic materials have definite porosities. The reaction kinetics and mass transfer are greatly enhanced as the metallic melt penetrates the refractory through the pores. The situation is further complicated by interfacial phenomena, which, in turn, would be affected by the dissolved elements in steel. These aspects are important in developing a futuristic model for the reactions between the runners and the steel melts.

V. SUMMARY AND CONCLUSIONS

The reactions between molten iron containing different amounts of oxygen and refractory materials that form part of the runners were investigated with a view to understand the mechanisms underlying the erosion phenomena and inclusion formation in the melt. A thermodynamic analysis of the reactions between Fe-O melts and Al_2O_3 , SiO_2 and mullite were carried out. "Finger experiments" were carried out wherein rods of the above-mentioned materials were dipped into the iron bath containing different amounts of oxygen for definite intervals of time. The samples were taken out and examined by Scanning Electron Microscope.

The results reveal that, in the case of Al_2O_3 in contact with oxygen saturated iron melts, an intermediate layer of ferroaluminate was getting formed. Corresponding experiments with quartz rod led toward the deforming of the rod with partial melting. The mullite reactions were expected to lead to somewhat similar results. The results are discussed on the basis of the thermodynamics of the reactions as well as from the viewpoint of the formation of inclusions in the iron melt.

VI. ACKNOWLEDGEMENTS

The present authors are extremely thankful to Dr. Du Sichen for useful discussions. The authors are also grateful to Dr. Vijaya Agarwala, TFR visiting professor at the Department of Materials Science, Royal Institute of Technology as well as Mr. Hans Bergqvist, for their help in carrying out the SEM analyses. Financial support for this work from Brinell Centre, KTH is gratefully acknowledged.

VII. REFERENCES

1. I. Barin, Thermodynamical Data of Pure Substances, Part I and II, VCH, 1993
2. D. R. Gaskell, Introduction to Metallurgical Thermodynamics, Taylor and Francis, 1981
3. T. Sjöqvist and P. Jönsson, Effect of Ferromanganese Additions on Inclusion Characteristic in Steel, TRITA-MET 043, 1999
4. P. Zhang, T. DebRoy, T and S. Seetharaman, Interdiffusion in the system MgO-Al₂O₃, *Metall. Materi. Trans.*, vol 27 A (1996), pp. 2105-14

VIII. FIGURE CAPTIONS

Fig 1. Phase diagram for the system Al-Fe-O

Fig 2. Stability diagram for the system Fe-O-Al, calculated values

Fig 3. Phase diagram for the system Fe-Si-O

Fig 4. Stability diagram for the system Fe-O-Si, calculated values

Fig 5. The apparatus used for the study of the erosion of refractory materials by molten metal.

Fig 6. The sampler holder

Fig 7. SEM analysis of Al₂O₃, 5 wt% Q, 2 h

Fig 8. SEM analysis of top bright layer, EDS mapping of point 1.

Fig 9. SEM analysis of Al₂O₃, 1.91 wt% Q, 40 h

Fig 10. SEM analysis of SiO₂, 0.2 wt% Q, 72 h.

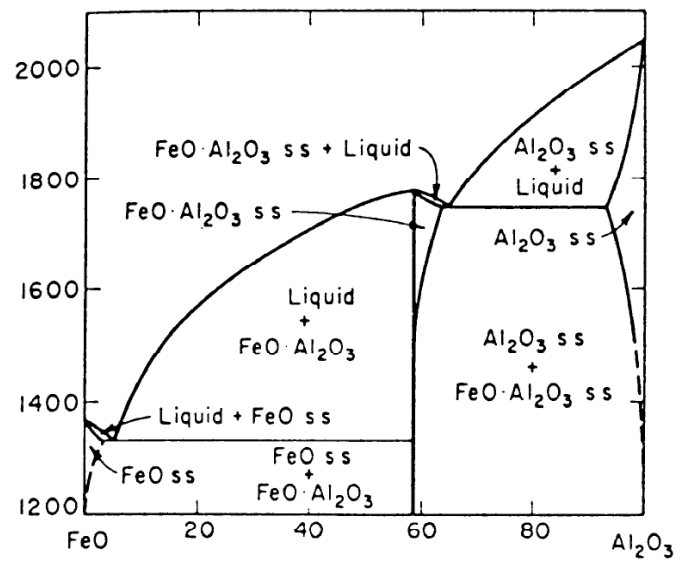


Fig 1. Phase diagram for the system Al-Fe-O

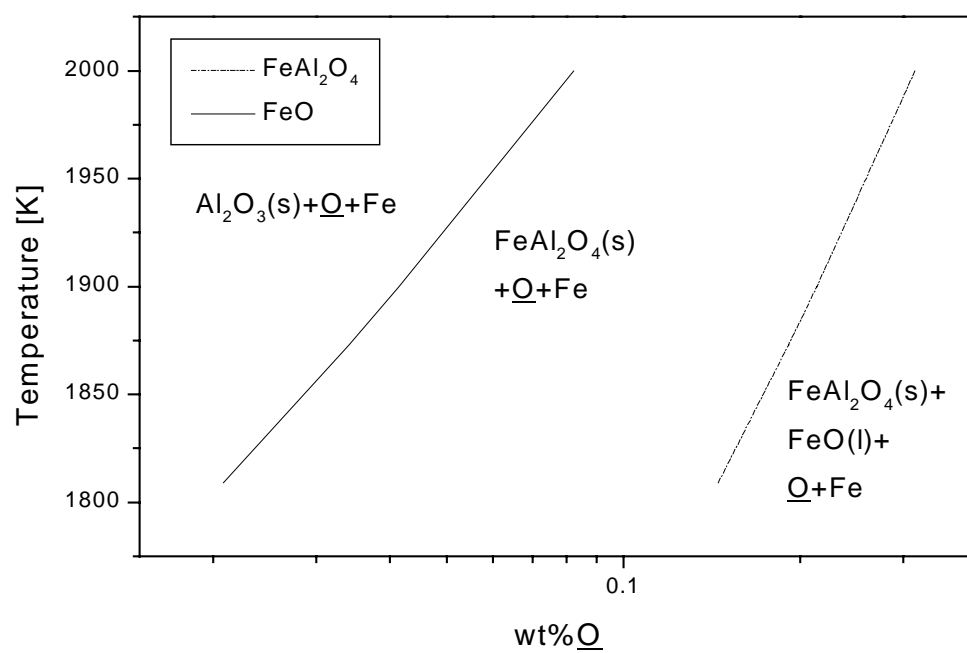


Fig 2. Stability diagram for the system Fe-O-Al, calculated values

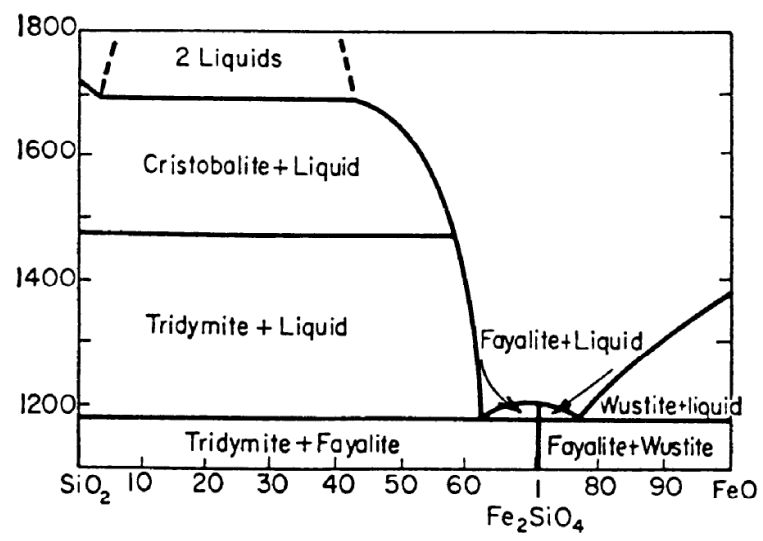


Fig 3. Phase diagram for the system Fe-Si-O

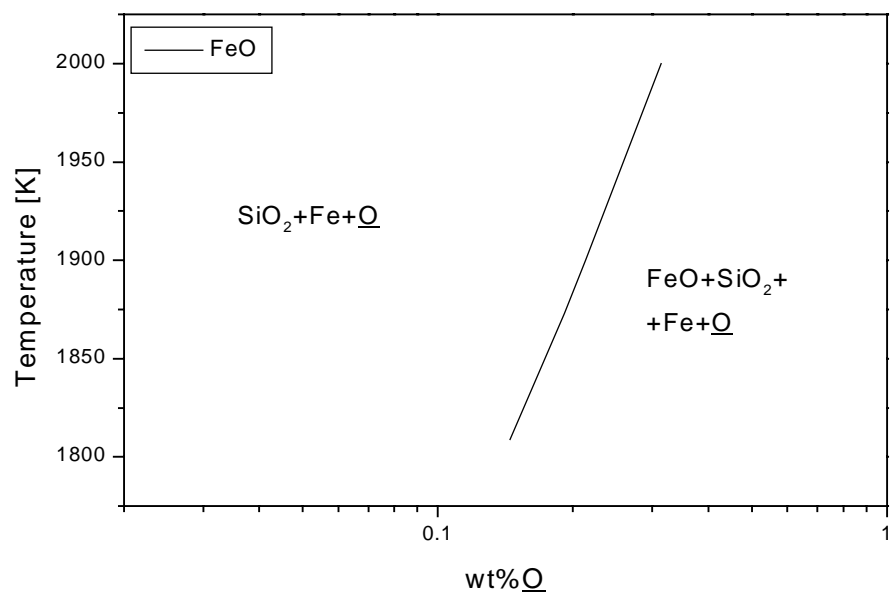


Fig 4. Stability diagram for the system Fe-O-Si, calculated values

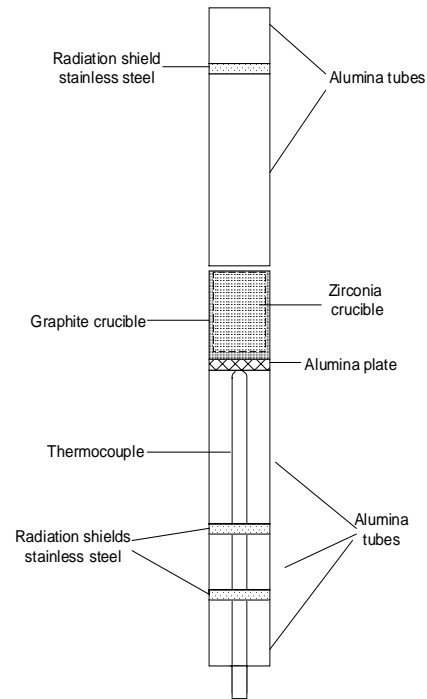


Fig 5. The apparatus used for the study of the erosion of refractory materials by molten metal.

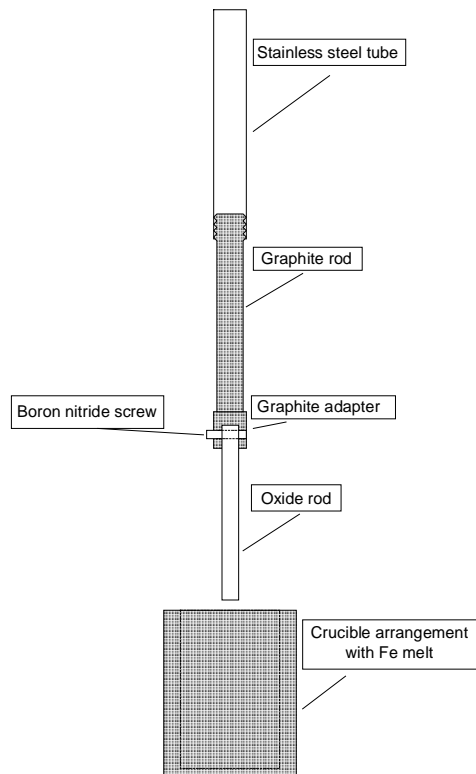


Fig 6. The sampler holder

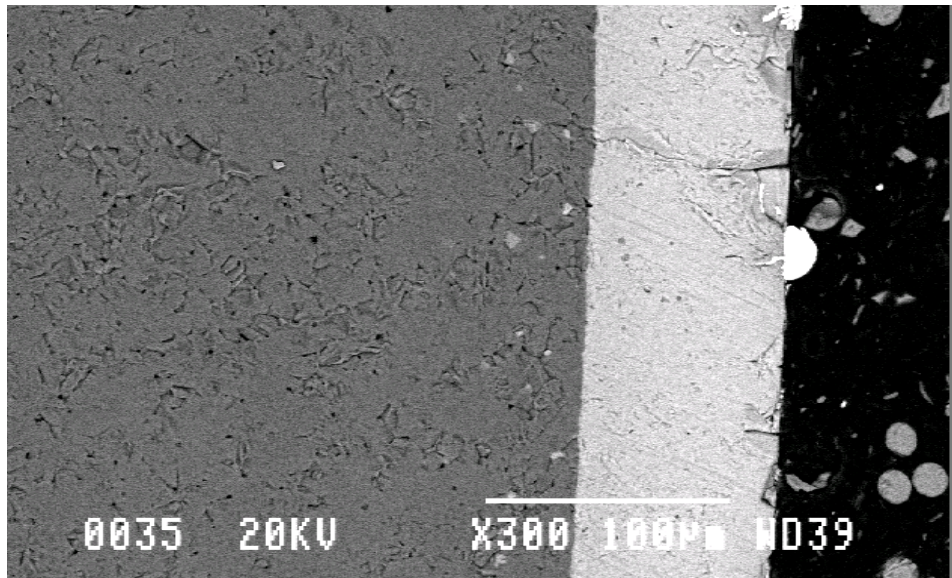


Fig 7. SEM analysis of Al_2O_3 , 5 wt% Q, 2 h

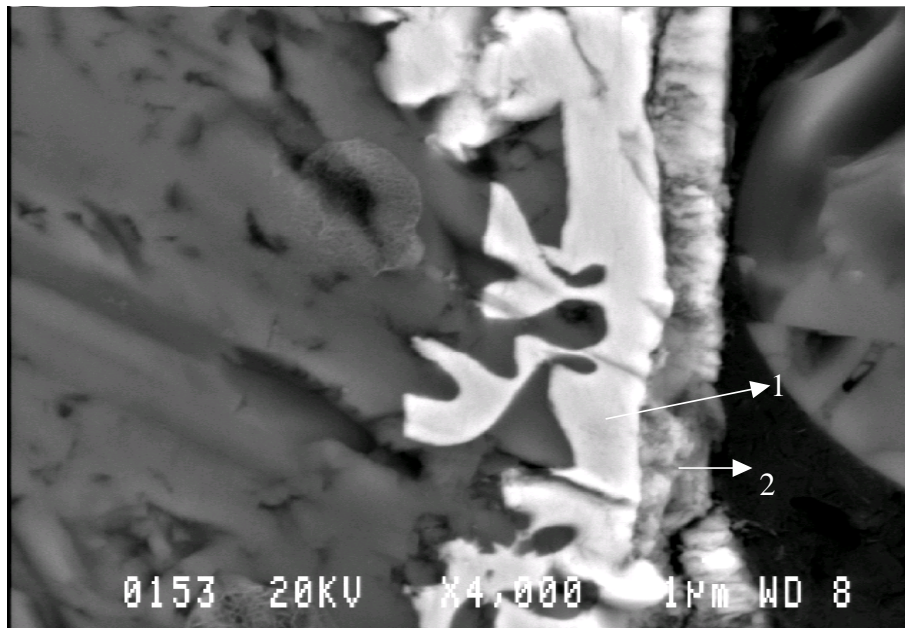


Fig 8. SEM analysis of top bright layer, EDS mapping of point 1 and 2.

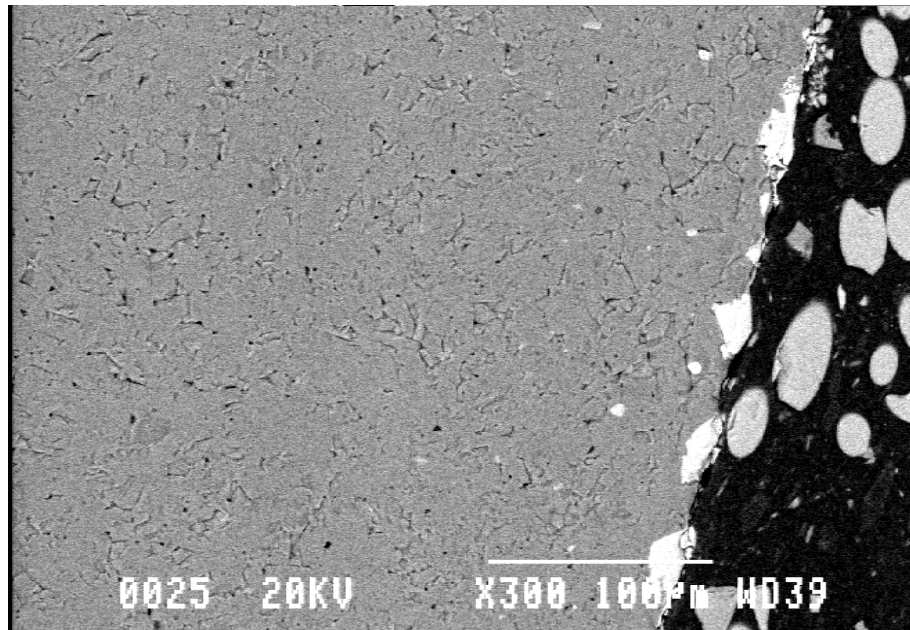


Fig 9. SEM analysis of Al_2O_3 , 1.91 wt% Q , 40 h

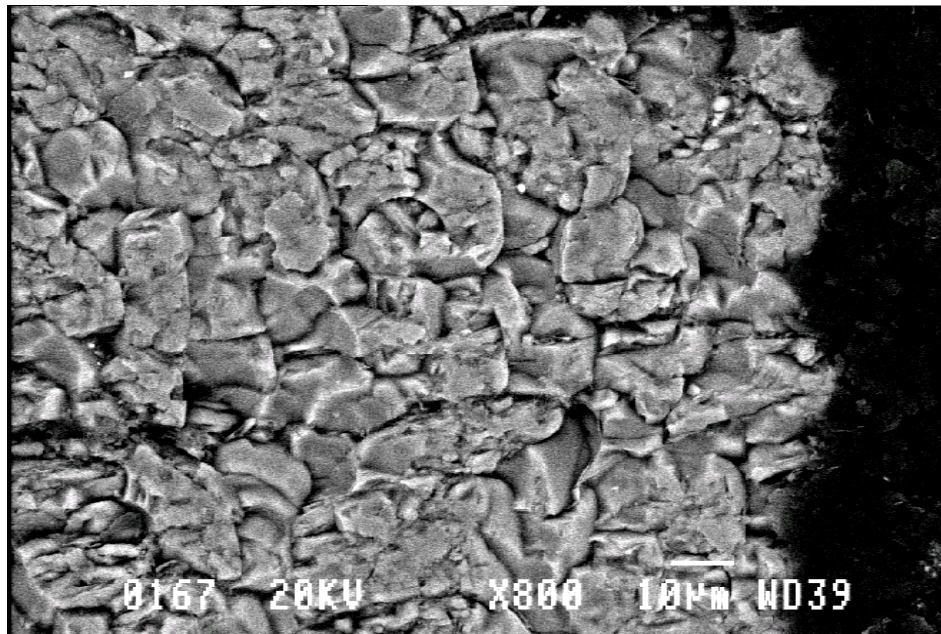


Fig 10. SEM analysis of SiO_2 , 0.2 wt% Q, 72 h.

IX. TABEL

Table I. X-ray fluorescence analysis of ARMCO iron³

Element	Wt %
C	0.0061
Si	0.0089
Mn	0.0644
P	0.0034
S	0.0032
Al	0.0019
Ni	0.0229
Cr	0.0105
V	0.0000
Mo	0.0000
Cu	0.0124
W	0.0011
Ti	0.0000
sum	0.13